Applied Physics Express

LETTERS

# Performance improvement of ohmic contacts on Al-rich n-AlGaN grown on single crystal AlN substrate using reactive ion etching surface treatment

To cite this article: Biplab Sarkar *et al* 2017 *Appl. Phys. Express* **10** 071001

Applied Physics Express **10**, 071001 (2017)
https://doi.org/10.7567/APEX.10.071001

# Performance improvement of ohmic contacts on Al-rich n-AlGaN grown on single crystal AlN substrate using reactive ion etching surface treatment

Biplab Sarkar[1*], Brian B. Haidet[1], Pramod Reddy[1,2], Ronny Kirste[1,2], Ramon Collazo[1], and Zlatko Sitar[1,2]

[1]Department of Materials Science and Engineering, North Carolina State University, Raleigh, NC 27695-7919, U.S.A.
[2]Adroit Materials, Cary, NC 27518, U.S.A.

*E-mail: bsarkar@ncsu.edu

Received May 4, 2017; accepted May 17, 2017; published online June 6, 2017

Four orders of magnitude improvement in specific contact resistivity of Al-rich n-AlGaN grown on single crystal AlN substrates is achieved by surface treatment based on reactive ion etching (RIE). The ohmic contacts to as-grown Al-rich n-AlGaN/AlN exhibit a high contact resistance and nonlinearity due to a large Schottky barrier and low dislocation density. The RIE surface treatment reduces the barrier height at the free surface by ∼0.5 eV and is also expected to introduce a defective surface required for ohmic contact formation.


With a variety of promising applications in UV optoelectronics[1–3] and power electronics,[4,5] Al-rich AlGaN has recently received great attention. Specifically, the high-quality, low-defect films that can be grown on single crystal AlN substrates with dislocation densities $<10^4\,cm^{-2}$[6,7] are enabling optoelectronic devices to perform in the deep-UV part of the spectrum.[8–10] AlGaN films grown on AlN substrates show carrier densities that are orders of magnitude higher than those of AlGaN films grown on sapphire substrates.[11] According to the Braslau alloyed contact model,[12] which depicts the inverse relationship between contact resistance and free carrier density, one should expect a better contact formation with AlGaN/AlN films compared to AlGaN/sapphire. However, the high quality of AlGaN/AlN films results in a highly resistive contact performance at low applied bias. Previously, it has been shown that ohmic contacts to AlGaN/AlN films exhibit nonlinear current–voltage ($I$–$V$) characteristics owing to bias-dependent current conduction regimes.[13] At lower applied bias, the conduction current is dominated by Frenkel–Poole (FP) defect-assisted tunneling whereas Fowler–Nordheim (FN) tunneling dominates at higher applied bias. Because of the absence of defects, the defect-assisted tunneling current is limited in AlGaN/AlN films, resulting in very low currents at low applied bias. Thus, the contact performance is poor at low applied bias conditions.

In this Letter, we report on further improvements of ohmic contacts to Al-rich n-type AlGaN/AlN films via reactive ion etching (RIE). A V/Al-based metallization scheme, which has been reported to outperform the traditional Ti/Al-based metallization scheme for Al-rich AlGaN,[14,15] has been used to characterize the contact formation. A significant improvement in the current resulting from FP defect-assisted tunneling at low applied bias is achieved after the RIE treatment. A comparison study with n-type AlGaN/sapphire films, where the defect-assisted tunneling current is higher owing to the presence of higher dislocation densities, is also presented. It is shown that the RIE-etched AlGaN/AlN surface shows contact resistance similar to that of an AlGaN/sapphire free surface at low applied bias, but outperforms the AlGaN/sapphire films by more than an order of magnitude at higher bias. A reduction in the Schottky barrier height at the AlGaN/AlN surface after the RIE surface treatment is thought to be a major contributor to the increase in defect-assisted tunneling current.

A 700 nm thick layer of n-$Al_{0.7}Ga_{0.3}N$ was grown on single crystal AlN substrates by metal organic chemical vapor deposition (MOCVD). Trimethylaluminum, triethylgallium, and ammonia gas were used as the Al, Ga, and N precursors, respectively. The film was doped with Si using silane as the precursor gas. Further details on MOCVD growth of n-AlGaN on single crystal AlN substrates can be found elsewhere.[7,16]

Initially, the n-AlGaN surface was cleaned with acetone, methanol, and deionized water for organic contamination removal, followed by dipping the sample in hot 1 : 1 HCl : $H_2O$ acid solution. Before depositing contacts using the transmission line method (TLM), part of the sample was etched in an RIE chamber using $SiCl_4$- and $Cl_2$-based chemistry.[17] The RIE process time was optimized to remove ∼15 nm of the n-AlGaN layer. Contacts were then deposited on the unetched (free surface) as well as the etched surface via electron-beam evaporation and conventional photolithography process. The contact metal stack consisted of 30 nm of V, 100 nm of Al, 70 nm of Ni, and 70 nm of Au. The contacts underwent rapid thermal annealing in $N_2$ atmosphere at 850 °C for 60 s. Individual rows of TLM contacts were isolated with a mesa etch achieved by RIE through the entire AlGaN layer. The $I$–$V$ characteristics of the TLM pads were recorded using a Keithley 4200 SCS. Analysis of specific contact resistivity was completed in MATLAB to characterize contacts with nonlinear $I$–$V$ characteristics.

Commonly, ohmic contacts to n-AlGaN are formed by depositing Ti/Al- or V/Al-based metal stacks and alloying the metals via rapid thermal annealing, leading to a reaction between the metal and AlGaN at the interface. A metal–nitride formation leaving behind nitrogen vacancies that act as donors at the metal–semiconductor interface after the contact anneal is believed to be responsible for the ohmic contact behavior.[18–20] Surface treatment before contact metal deposition strongly influences the behavior of the ohmic contacts to Al-rich AlGaN, as shown in Fig. 1. Figure 1(a) shows a comparison of the $I$–$V$ characteristics of TLM contacts on n-type $Al_{0.7}Ga_{0.3}N$ grown on AlN substrates between the unetched (free surface) and the RIE-etched surface. Previous studies have shown that nonlinear $I$–$V$ characteristics are commonly observed in Al-rich n-type AlGaN/AlN films.[13] Such a diode-type behavior can be understood as follows: FP defect-assisted tunneling, which is dominant at low applied bias, is limited owing to presence of fewer defects in AlGaN/AlN films. After a certain applied bias (represented as $V_1$

 

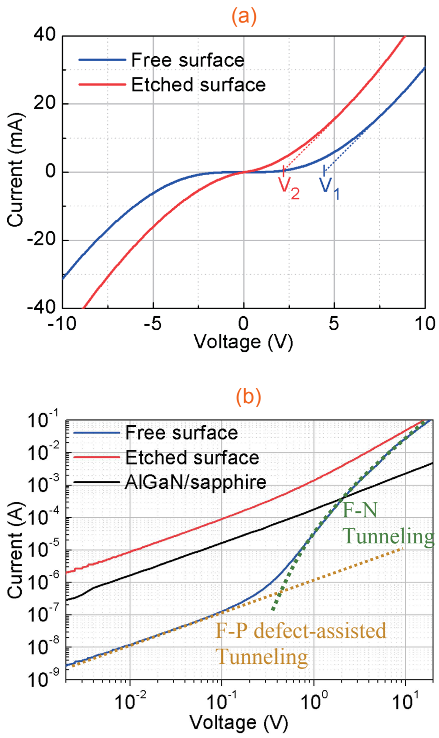


**Fig. 1.** (a) *I–V* characteristics of TLM contacts (with a pad spacing of ~15 µm) on the free and RIE-etched surface of n-AlGaN/AlN. (b) *I–V* characteristics on a log–log scale showing the significant increase in current for the etched surface at low bias voltages. A comparison with contacts to n-AlGaN grown on sapphire substrates is also shown.

for the free surface), FN tunneling dominates and current through the contact is eventually limited by the sheet resistance. By comparing the *I–V* curves in Fig. 1(a), it is found that the etched surface requires a much lower voltage ($V_2 \approx 2.2$ V vs $V_1 \approx 4.5$ V) to reach the sheet resistance dominant conduction regime than the free surface.

A better insight into the different conduction regimes can be obtained by plotting the *I–V* characteristics on a log–log scale, as shown in Fig. 1(b). For the *I–V* characteristics for an AlGaN/AlN free surface, a straight line at low applied bias represents the current through FP defect-assisted tunneling; this is followed by a sharp increase in current resulting from FN tunneling at higher bias.[13] For comparison, the performance of a V/Al-based ohmic contact on the free surface of AlGaN/sapphire film with similar composition is also presented. The defect-assisted tunneling current is much higher for films grown on a sapphire substrate owing to the much higher dislocation density.[13] However, RIE treatment of the AlGaN/AlN surface results in defect-assisted tunneling several orders of magnitude higher than that for the free surface and also higher than that for the AlGaN/sapphire films. Note that the defect-assisted tunneling current increases with increasing temperature, whereas FN tunneling should be independent of temperature for Al-rich AlGaN with a high barrier at the metal–semiconductor interface.[21] Figure 2 shows the temperature-dependent *I–V* characteristics of the V/Al contact on the etched AlGaN/AlN surface. Strong temperature dependence at lower applied bias confirms that defect-assisted tunneling is dominant in the RIE-etched AlGaN/AlN surface as well. Thus, the improvement in contact performance at low applied bias can be attributed to the increase in defect-assisted tunneling after RIE surface treatment.

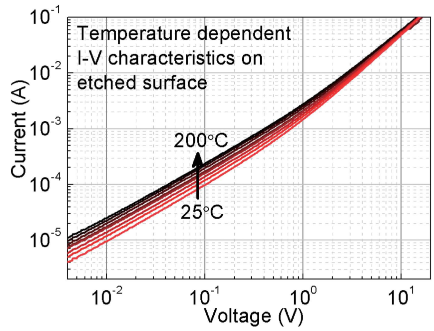


**Fig. 2.** Temperature-dependent *I–V* characteristics of ohmic contact to an RIE-etched AlGaN/AlN surface taken at 25 °C increments.

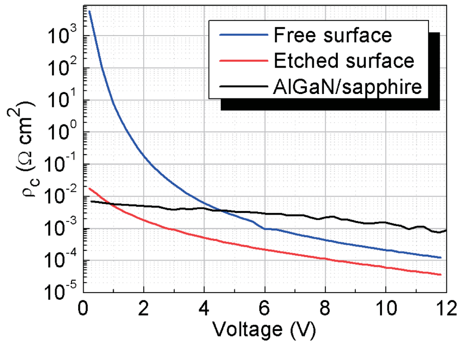


**Fig. 3.** Comparison of specific contact resistivity ($\rho_c$) between free AlGaN/AlN and etched AlGaN/AlN surfaces. For comparison, $\rho_c$ for an AlGaN/sapphire free surface is also shown. Note that specific contact resistivity is known to decrease with applied voltage for nonlinear TLM contacts.[23,24]

The effect of RIE surface treatment on contact resistance was further studied by using the method developed by Piotrzkowski et al. for nonlinear TLM contacts.[22] Specific contact resistivity was calculated as a function of applied voltage for the free and RIE-etched AlGaN/AlN surfaces, as well as for AlGaN/sapphire film, as shown in Fig. 3. At low bias, the AlGaN/sapphire films show higher current than unetched AlGaN/AlN films, resulting in a better contact performance for AlGaN/sapphire films. However, RIE surface treatment of AlGaN/AlN film reduces the specific contact resistivity by ~4 orders of magnitude at low applied bias. At higher bias, both the free and etched AlGaN/AlN films show superior contact performance compared to AlGaN/sapphire films owing to the presence of higher carrier densities. This indicates the necessity of growing AlGaN/AlN films for future device applications in which a minimal contact resistance is desirable. Further improvement in contact performance for AlGaN/AlN films is thus obtained by performing a surface treatment with RIE.

To identify factors leading to such increases in defect assisted tunneling on the etched AlGaN surface, the effect of etching on the surface states, Fermi level pinning, barrier height, and surface chemical composition were studied via X-ray photoelectron spectroscopy (XPS). The procedure employed to determine the surface Fermi level and the corresponding barrier height on III–nitride free surfaces by XPS is described elsewhere.[21,25] In particular, it has to be noted that the core shell binding energies are measured with respect to the Fermi level and the energy difference between the valence band maximum and a core shell's binding energy

 

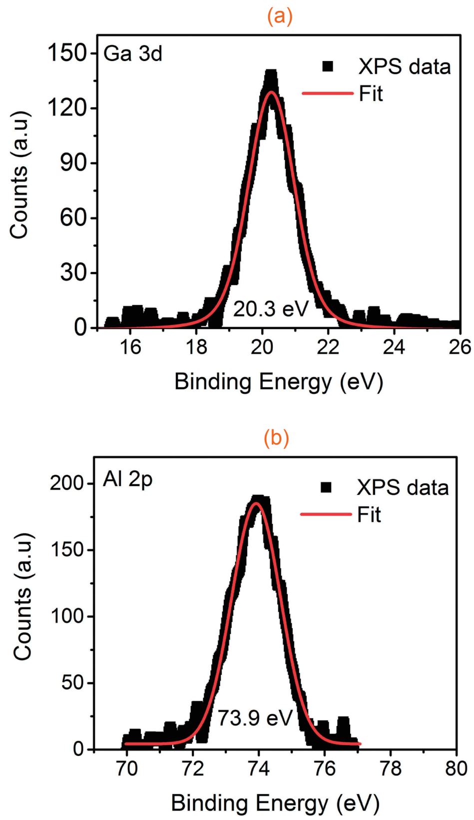


**Fig. 4.** Core shell binding energies of (a) Ga 3d and (b) Al 2p at $SiCl_4$ etched n-$Al_{0.7}Ga_{0.3}N$.

remains constant for a particular Al composition. Hence, any shift in the Fermi level with respect to the valence band maximum (i.e., barrier height or Fermi level pinning energy) as a result of surface modifications or interface formation by etching, passivation, or Schottky contact formation is reflected in a corresponding shift in the core shell binding energy.[26,27] As deposited, *c*-plane n-$Al_{0.7}Ga_{0.3}N$ showed a free surface barrier height (at the charge neutrality level), i.e., Fermi level pinning, at 1.8 eV and the corresponding Al 2p and Ga 3d core levels had binding energies of ~73.5 and 19.7 eV, respectively, in agreement with earlier results.[21] In contrast, etching of the surface increases the Ga 3d and Al 2p core shell binding energies by ~0.5 eV and hence reduces the barrier height to ~1.3 eV, as shown in Fig. 4. The decrease in barrier height is in agreement with the large increase in the injection-limited defect-assisted tunneling current[13] shown in Fig. 1(b). Other factors such as introduction of a defective surface after RIE treatment, increase in effective contact area, and removal of surface oxide, etc.[20] could also contribute to the defect-assisted tunneling current. However, it is very unlikely that these factors can increase the defect-assisted tunneling current by several orders of magnitude. Thus, the major contributor to the increase in current at low voltages in AlGaN/AlN films can be attributed to the reduced barrier height at the metal–semiconductor interface after RIE surface treatment.

In conclusion, we reported the performance improvement of ohmic contacts to Al-rich n-AlGaN grown on a single crystal AlN substrate by RIE surface treatment. Contacts to Al-rich n-$Al_{0.7}Ga_{0.3}N$ films grown on single crystal AlN substrates exhibit a large Schottky barrier (~1.8 eV), resulting in a nonlinear current–voltage relationship. The RIE treatment of a defect-free surface prior to contact metallization lowered the specific contact resistivity by several orders of magnitude at a low bias. The main contribution to this improvement was found to be a significant reduction in the barrier height at the free surface (by ~0.5 eV) after RIE treatment. The introduction of a defective surface after the RIE treatment may also play a role in reducing the specific contact resistivity.

**Acknowledgments** We are sincerely grateful for the support from NSF (ECCS-1508854, ECCS-1610992, DMR-1508191, and ECCS-1653383) and ARO (W911NF-15-2-0068 and W911NF-16-C-0101) for funding this work.

1) M. Kneissl, in *III–Nitride Ultraviolet Emitters*, ed. M. Kneissl and J. Rass (Springer, Cham, 2016) p. 1.
2) A. Khan, K. Balakrishnan, and T. Katona, Nat. Photonics **2**, 77 (2008).
3) K. H. Li, X. Liu, Q. Wang, S. Zhao, and Z. Mi, Nat. Nanotechnol. **10**, 140 (2015).
4) R. J. Kaplar, A. A. Allerman, A. M. Armstrong, M. H. Crawford, J. R. Dickerson, A. J. Fischer, A. G. Baca, and E. A. Douglas, ECS J. Solid State Sci. Technol. **6**, Q3061 (2017).
5) J. Xie, S. Mia, R. Dalmau, R. Collazo, A. Rice, J. Tweedie, and Z. Sitar, Phys. Status Solidi C **8**, 2407 (2011).
6) R. Dalmau, B. Moody, R. Schlesser, S. Mita, J. Xie, M. Feneberg, B. Neuschl, K. Thonke, R. Collazo, A. Rice, J. Tweedie, and Z. Sitar, J. Electrochem. Soc. **158**, H530 (2011).
7) I. Bryan, Z. Bryan, S. Mita, A. Rice, L. Hussey, C. Shelton, J. Tweedie, J.-P. Maria, R. Collazo, and Z. Sitar, J. Cryst. Growth **451**, 65 (2016).
8) J. Xie, S. Mita, Z. Bryan, W. Guo, L. Hussey, B. Moody, R. Schlesser, R. Kirste, M. Gerhold, R. Collazo, and Z. Sitar, Appl. Phys. Lett. **102**, 171102 (2013).
9) W. Guo, Z. Bryan, J. Xie, R. Kirste, S. Mita, I. Bryan, L. Hussey, M. Bobea, B. Haidet, M. Gerhold, R. Collazo, and Z. Sitar, J. Appl. Phys. **115**, 103108 (2014).
10) Z. Ren, Q. Sun, S.-Y. Kwon, J. Han, K. Davitt, Y. K. Song, A. V. Nurmikko, W. Liu, J. Smart, and L. Schowalter, Phys. Status Solidi C **4**, 2482 (2007).
11) R. Collazo, S. Mita, J. Xie, A. Rice, J. Tweedie, R. Dalmau, and Z. Sitar, Phys. Status Solidi C **8**, 2031 (2011).
12) N. Braslau, J. Vac. Sci. Technol. **19**, 803 (1981).
13) B. B. Haidet, I. Bryan, P. Reddy, Z. Bryan, R. Collazo, and Z. Sitar, J. Appl. Phys. **117**, 245702 (2015).
14) R. France, T. Xu, P. Chen, R. Chandrasekaran, and T. D. Moustakas, Appl. Phys. Lett. **90**, 062115 (2007).
15) J. H. Wang, S. E. Mohney, S. H. Wang, U. Chowdhury, and R. D. Dupuis, J. Electron. Mater. **33**, 418 (2004).
16) Z. Bryan, I. Bryan, B. E. Gaddy, P. Reddy, L. Hussey, M. Bobea, W. Guo, M. Hoffmann, R. Kirste, J. Tweedie, M. Gerhold, D. L. Irving, Z. Sitar, and R. Collazo, Appl. Phys. Lett. **105**, 222101 (2014).
17) E. Zhirnov, S. Stepanov, W. N. Wang, Y. G. Shreter, D. V. Takhin, and N. I. Bochkareva, J. Vac. Sci. Technol. A **22**, 2336 (2004).
18) M. W. Fay, G. Moldovan, N. J. Weston, P. D. Brown, I. Harrison, K. P. Hilton, A. Masterton, D. Wallis, R. S. Balmer, M. J. Uren, and T. Martin, J. Appl. Phys. **96**, 5588 (2004).
19) D. H. Zadeh, S. Tanabe, N. Watanabe, and H. Matsuzaki, Jpn. J. Appl. Phys. **55**, 05FH06 (2016).
20) S. Ruvimov, Z. Liliental-Weber, J. Washburn, K. J. Duxstad, E. E. Haller, Z.-F. Fan, S. N. Mohammad, W. Kim, A. E. Botchkarev, and H. Morkoç, Appl. Phys. Lett. **69**, 1556 (1996).
21) P. Reddy, I. Bryan, Z. Bryan, J. Tweedie, S. Washiyama, R. Kirste, S. Mita, R. Collazo, and Z. Sitar, Appl. Phys. Lett. **107**, 091603 (2015).
22) R. Piotrzkowski, E. Litwin-Staszewska, and S. Grzanka, Appl. Phys. Lett. **99**, 052101 (2011).
23) M. Oh, W.-Y. Jin, H. J. Jeong, M. S. Jeong, J.-W. Kang, and H. Kim, Sci. Rep. **5**, 13483 (2015).
24) Y. Gil and H. Kim, Thin Solid Films **603**, 307 (2016).
25) P. Reddy, I. Bryan, Z. Bryan, W. Guo, L. Hussey, R. Collazo, and Z. Sitar, J. Appl. Phys. **116**, 123701 (2014).
26) P. Reddy, S. Washiyama, F. Kaess, M. Hayden Breckenridge, L. H. Hernandez-Balderrama, B. B. Haidet, D. Alden, A. Franke, B. Sarkar, E. Kohn, R. Collazo, and Z. Sitar, J. Appl. Phys. **119**, 145702 (2016).
27) P. Reddy, I. Bryan, Z. Bryan, J. Tweedie, R. Kirste, R. Collazo, and Z. Sitar, J. Appl. Phys. **116**, 194503 (2014).